MOLECULAR AND CELLULAR BIOLOGY, Jan. 1995, p. 35–44 Vol. 15, No. 1
0270-7306/95/$04.00+0

Alternative Translation of Human Fibroblast Growth Factor 2 mRNA Occurs by Internal Entry of Ribosomes

STÉPHAN VAGNER,[1] MARIE-CLAIRE GENSAC,[1] ARLETTE MARET,[1] FRANCIS BAYARD,[1] FRANÇOIS AMALRIC,[2] HERVÉ PRATS,[1] AND ANNE-CATHERINE PRATS[1]*

INSERM U397, Endocrinologie et Communication Cellulaire, Institut Louis Bugnard, Centre Hospitalier Universitaire de Rangueil, 31054 Toulouse Cedex,[1] and Laboratoire de Biologie Moléculaire Eucaryote du Centre National de la Recherche Scientifique, 31062 Toulouse Cedex,[2] France

Received 27 June 1994/Returned for modification 7 September 1994/Accepted 23 September 1994

Alternative initiations of translation of the human fibroblast growth factor 2 (FGF-2) mRNA, at three CUG start codons and one AUG start codon, result in the synthesis of four isoforms of FGF-2. This process has important consequences on the fate of FGF-2: the CUG-initiated products are nuclear and their constitutive expression is able to induce cell immortalization, whereas the AUG-initiated product, mostly cytoplasmic, can generate cell transformation. Thus, the different isoforms probably have distinct targets in the cell. We show here that translation initiation of the FGF-2 mRNA breaks the rule of the cap-dependent ribosome scanning mechanism. First, translation of the FGF-2 mRNA was shown to be cap independent in vitro. This cap-independent translation required a sequence located between nucleotides (nt) 192 and 256 from the 5′ end of the 318-nt-long 5′ untranslated region. Second, expression of bicistronic vectors in COS-7 cells indicated that the FGF-2 mRNA is translated through a process of internal ribosome entry mediated by the mRNA leader sequence. By introducing additional AUG codons into the RNA leader sequence, we localized an internal ribosome entry site to between nt 154 and 318 of the 5′ untranslated region, just upstream of the first CUG. The presence of an internal ribosome entry site in the FGF-2 mRNA suggests that the process of internal translation initiation, by controlling the expression of a growth factor, could have a crucial role in the control of cell proliferation and differentiation.

Fibroblast growth factor 2 (FGF-2), also known as basic fibroblast growth factor, belongs to a family of cytokines able to promote proliferation of neuroectodermal and epithelial cells as well as differentiation of mesenchymal cells. FGF-2 is also an angiogenic factor involved in wound-healing processes (18, 45) such as salvage of infarcted myocardium (56) and also in tumor neovascularization (25). FGF-2 is synthesized by a wide variety of cells, including endothelial cells (48). In these cells, several forms of FGF-2 are detected, resulting from alternative initiations of translation at three CUG start codons and one AUG start codon (14, 42). The process of alternative initiation of translation has many consequences for the fate of FGF-2. The CUG-initiated forms contain a nuclear localization sequence (9) and are mostly recovered in the nucleus (44). In contrast, the AUG-initiated form, lacking a nuclearization sequence, is mostly cytosolic, although it is sometimes also nuclear (8, 9). Moreover, the CUG- and AUG-initiated forms of FGF-2 can influence cell behavior differently. Constitutive expression of the AUG-initiated form leads to transformation of adult bovine aortic endothelial and NIH 3T3 cells, whereas expression of the CUG-initiated forms leads to immortalization of adult bovine aortic endothelial cells and to slower growth of NIH 3T3 cells (11, 43).

The process of alternative initiation of translation involves a growing number of viral and cellular mRNAs ranging from yeasts to humans. The choice of initiation codon often determines the subcellular fate and the function of the protein: for instance, the use of alternative codons gives rise to a cell membrane antigen versus a virion capsid precursor, to a nuclear versus a secreted protein, or to a mitochondrial versus a cytosolic/nuclear enzyme in the case of murine leukemia virus (40), FGF-3 (1), or yeast MOD5 (49) mRNA, respectively. Then the process of alternative initiation of translation not only increases gene diversity but also can control the relative expression of proteins with different locations and functions encoded by a same mRNA.

In eukaryotic cells, translation is thought to be initiated by a ribosome scanning from the capped mRNA 5′ end, under the control of initiation factors (27, 50). This model states that the 40S ribosomal subunit initially binds to the mRNA 5′ cap structure and then migrates along the mRNA molecule in the 3′ direction until it recognizes an AUG codon in a favorable context. Regulation of translation mostly occurs at the initiation level (51), and each initiation step is a target for translational control. Several *cis*-acting elements, including the cap structure, secondary structures in the mRNA 5′ untranslated region (UTR), the consensus sequence flanking the start codon and the presence of a noncanonical codon, are involved.

The process of ribosome binding to the cap structure is the limiting step of translation initiation, as the cap-binding eukaryotic initiation factor 4E (eIF-4E) is present in only low amounts in cells (13, 19). When overexpressed, this factor induces malignant transformation of NIH-3T3 cells (30) and deregulation of HeLa cell growth (12). eIF-4E has been shown to enhance unefficient translation of mRNAs that contain extensive secondary structures in their 5′ UTRs (26). Thus, the transforming effect of eIF-4E may result from a translational derepression of mRNAs coding for proteins involved in the control of cell growth and differentiation. Indeed, oncoproteins, transcription factors, and growth factors mRNAs possess long G+C-rich 5′ UTRs (28). All of these observations indicate that the regulation of translation initiation plays a central role in the control of cell proliferation.

* Corresponding author. Mailing address: INSERM U397, Endocrinologie et Communication Cellulaire, Institut Louis Bugnard, C.H.U. Rangueil, Avenue Jean Poulhès, 31054 Toulouse Cedex, France.

An alternative ribosome binding pathway, independent of the cap structure and of eIF-4E, has also been evidenced (20): an internal ribosome entry site (IRES) has been found in all picornaviruses examined to date, including enteroviruses such as poliovirus and hepatitis A virus (17, 38), cardiovirus (22, 24), aphthovirus (2, 4, 29), and rhinovirus (7), the mRNAs of which are devoid of cap structure and possess a long 5′ UTR (600 to 1,200 nucleotides [nt]) with multiple cryptic AUG codons. This process of internal initiation of translation has also been reported for other types of virus, i.e., hepatitis C virus (54) and also a plant virus, cowpea mosaic virus (52), the genomes of which show similarities with that of picornavirus. Furthermore, for picornavirus mRNA, this process has been shown to depend on cellular *trans*-acting factors (23, 34), suggesting that it could also involve cellular mRNAs. This hypothesis has been confirmed by the recent demonstration of internal translation initiation occurring in the case of human immunoglobulin heavy-chain-binding protein and *Drosophila* Antennapedia mRNAs (32, 36).

We have recently shown that FGF-2 mRNA is not translated according to the eIF-4E-dependent scanning model (41). Mutation of the first or all three initiation CUGs into nonstart codons does not lead to an increase in initiation at the downstream start codons. Moreover, the 318-nt-long G+C rich 5′ UTR, which behaves as a strong translation inhibitor in the wheat germ extract, has no effect either in vitro in rabbit reticulocyte lysate (RRL) or in vivo in COS-7 cells. These observations prompted us to look for a possible IRES (21) in the FGF-2 mRNA. In this report, we show that initiation of FGF-2 mRNA translation is cap independent in RRL and that it occurs, in transfected COS-7 cells, through a process of internal ribosome entry, mediated by an IRES located upstream of CUG1.

MATERIALS AND METHODS

Plasmid construction. The constructs depicted in Fig. 1A were made in vector Bluescript KS+ (Stratagene) as previously described (41). Other constructs are detailed below. They were made in vector pSCT (46) with both cytomegalovirus and T7 promoters.

The FGF-chloramphenicol acetyltransferase (CAT) chimeric constructs are shown in Fig. 1B. The monocistronic plasmid pFC1 (encoding the FGF-CAT1 fusion) and derived constructs have been previously described (41). The pFC1 construct results from the fusion of nt 1 to 539 of FGF-2 cDNA to the CAT coding sequence. Plasmids pFC1-Δ312 and pFC1-Δ472 result from deletions of nt 1 to 312 and 1 to 472 of FGF-2 cDNA, respectively, in plasmid pFC1. The monocistronic plasmid pFC2 (encoding the FGF-CAT2 fusion) contains a fusion of nt 1 to 472 of FGF-2 cDNA with the CAT coding sequence and was constructed from the pSVL-derived plasmid pSC3 (9) as follows. The FGF-CAT2 fusion was introduced into vector pSCT by tripartite ligation of the *Apa*I-*Sac*I fragment (FGF-CAT sequence) of plasmid pSC3 with the *Xba*I-*Apa*I (5′ leader) and *Sac*I-*Xba*I (vector) fragments of plasmid pFC1. Plasmids pFC1-5′rev and pFC2-5′rev (with an inverted 5′ UTR) were derived from plasmids pFC1 and pFC2, respectively, by tripartite ligation of the *Xba*I-Klenow-*Xho*I fragment (5′ UTR) with the *Xho*I-Klenow-*Sac*I fragments (FGF-CAT sequences) and *Sac*I-*Sal*I (vector) fragments of plasmids pFC1 and pFC2, respectively.

Structures of bicistronic vectors are shown in Fig. 5A and 7A. The monocistronic plasmid pSCT-FGF, containing the complete FGF-2 cDNA sequence, has been previously described (41). The bicistronic plasmid pBI-FGF resulted from ligation of the *Nar*I-*Bgl*II (3′ region of FGF-2 cDNA plus part of the vector) fragment of plasmid pSCT-FGF with the *Nar*I-*Bgl*II (vector plus CAT plus 5′ region of FGF-2 cDNA) fragment of plasmid pBI-FC1. The bicistronic plasmid pBI-FC1 was constructed by tripartite ligation of the *Xba*I-*Pvu*I fragment of plasmid pFC1 (FGF-CAT1 fusion plus part of the vector) with the *Pvu*I-*Hin*dIII (other part of the vector) and *Hin*dIII-*Xba*I (CAT sequence) fragments of vector pSCT-CAT (41). The other bicistronic plasmids were constructed in a similar way, using the *Xba*I-*Pvu*I fragment of each corresponding monocistronic plasmid. In the bicistronic vectors, the first cistron (CAT) is preceded by a 134-nt-long leader when the cytomegalovirus promoter is used for transcription and by a 62-nt-long leader when the T7 promoter is used. A 106-nt-long spacer separates the first cistron from the FGF-2 cDNA residues. This spacer contains 11 stop codons, 7 of which are in frame with the first cistron.

A stable hairpin ($\Delta G = -40$ kcal [ca. −167 kJ]/mol, calculated by using PC Gene) was created by introduction of a double-stranded oligonucleotide (5′-AGCTTGGCGAGATTTTCAGGAGTCAG-3′ and 5′-GATCCTGACTCCTG AAAATCTCGCCA-3′) between the *Bam*HI and *Hin*dIII sites of plasmid pSCT-CAT, upstream of the CAT sequence. This was accomplished by tripartite ligation of the double-stranded oligonucleotide (sticky with *Bam*HI and *Hin*dIII ends) with the *Hin*dIII-*Xba*I (CAT) and *Xba*I-*Bam*HI (vector) fragments of plasmid pSCT-CAT. The pHP plasmid series was derived from the latter construct by using the same strategy as for the pBI plasmids (see above). In RNAs expressed from the pHP plasmids, the hairpin is located at the 5′ end for T7 RNAs but 72 nt from the 5′ end for cytomegalovirus RNAs.

Additional AUG codons (see Fig. 5A) were inserted by site-directed mutagenesis. An AUG was introduced at position 154 by PCR amplification of nt 1 to 181 of the 5′ UTR, using oligonucleotides 5′-GGGTCTAGACCGCCGAACTCAG GCCGGCCCCAGAAAACCCGAG-3′ (containing an *Xba*I site followed by nt 1 to 34) and 5′-GGGGATCCCGTTGCAACCGCGGGCAGC**AT**CCGCTA-3′ (complementary to nt 148 to 181, with an in-frame AUG introduced at position 154 [boldface], containing the *Bam*HI site at position 176). This fragment was introduced, using *Xba*I and *Bam*HI enzymes, into the monocistronic vector pFC1. Mutation of CUG1 (position 319) into AUG has been described previously (41).

Mutations were checked by DNA sequencing using the dideoxy method (47).

In vitro translation. Plasmids were linearized downstream from the 3′ end of the FGF-2 or FGF-CAT coding sequence. Capped or uncapped RNAs were generated in vitro by T7 or T3 RNA polymerase according to the manufacturer's instructions, with or without adding m^7GpppG (0.5 mM) to the transcription reaction mixture, respectively. RNA transcripts were quantitated by A_{260} and ethidium bromide staining on an agarose gel, which also allowed verification of their integrity. In vitro translation in RRL (Promega) was performed as previously described (41), in the presence of [^{35}S]methionine (Amersham). Translation products were analyzed by electrophoresis in a sodium dodecylsulfate (SDS)–12.5% polyacrylamide gel (47). Autoradiograms of the dried gels were scanned with a BIOCOM apparatus.

DNA transfection and Western immunoblotting (immunoblotting). COS-7 monkey cells were transfected by the DEAE-dextran method as described previously (41). Briefly, 0.5 or 1 μg of each plasmid was incubated with the cells for 20 min at 37°C in the presence of 1 mg of DEAE-dextran per ml, then chloroquine was added at 40 μg/ml, and incubation was continued for 4 h. The DNA was removed, and cells were incubated in 10% dimethyl sulfoxide for 2 min. Cell lysates were prepared 48 h later by scraping the cell monolayers. Cell pellets were frozen-thawed, resuspended in 0.1 M Tris (pH 7.8), and sonicated. Total proteins were quantified by the Bio-Rad assay (A_{595}) and 3 μg of proteins from each cell lysate was used for Western immunoblotting as previously described (41). In summary, lysates were heated for 2 min at 95°C in SDS- and dithiothreitol-containing sample buffer, separated in a 12.5% polyacrylamide gel, and transferred onto a nitrocellulose membrane. CAT and FGF-2 proteins were immunodetected with a rabbit polyclonal anti-CAT antibody prepared in the laboratory (1/50,000 dilution) and an anti-FGF-2 antibody (1/200 dilution; Oncogene Science), respectively. Antibodies were detected with an enhanced chemiluminescence kit (Amersham).

Cellular RNA purification. Total cellular RNA was prepared by the RNAzol B method (Bioprobe Systems), derived by the guanidinium thiocyanate procedure (10). A total of 5×10^6 transfected cells were scraped, centrifuged, and lysed in RNAzol (1 ml). RNA was extracted after chloroform addition (0.1 ml) and precipitated by isopropanol. Following an ethanol wash and precipitation, RNA was quantitated by measuring the A_{260} and checked for integrity by electrophoresis on an agarose gel and ethidium bromide staining. To eliminate DNA contamination, RNA was treated with 10 U of RNase-free DNase I for 30 min at 37°C.

RNase mapping. A complementary-strand RNA probe was generated in vitro by T7 RNA polymerase according to the manufacturer's instructions, using a linearized DNA template in the presence of 50 μCi of [α-^{32}P]CTP. ^{32}P-labelled RNA was purified by using an RNaid kit (Bio 101). The RNA probe was hybridized with total cellular RNA as previously described (47). Two micrograms of RNA was dissolved in 30 μl of hybridization buffer [80% formamide, 40 mM piperazine-*N*,N′-bis(2-ethanesulfonic acid) (PIPES; pH 6.4), 400 mM NaCl, 1 mM EDTA] containing a 20-fold excess of probe (2×10^5 cpm), heated at 90°C for 15 min, and incubated at 45°C for 8 h; 500 μl of 10 mM Tris-HCl (pH 7.5)–5 mM EDTA–300 mM NaCl containing 40 μg of RNase A and 2 μg of RNase T_1 per ml was added, and the reaction mixture was incubated for 1 h at 37°C. After addition of 50 μg of proteinase K and 10 μl of 20% SDS, the mixture was incubated for 15 min at 37°C and then subjected to phenol extraction and ethanol precipitation with carrier tRNA. The RNA samples were then dissolved, denatured, and fractionated on a 6% polyacrylamide-urea gel at 15 V/cm. The gel was dried and autoradiographed.

Northern (RNA) blotting. Northern blotting was performed as previously described (47). DNA probes were labelled with [^{32}P]dATP by using a nick translation kit provided by Promega. Total cellular RNA (1 μg per lane) was subjected to electrophoresis through 1.2% formaldehyde–agarose gels at 4 V/cm (in 40 mM morpholinepropanesulfonic acid [MOPS; pH 7]–5 mM sodium acetate–1 mM EDTA) and electrotransferred to a nylon membrane (2 h at 500 mA in 25 mM sodium phosphate [pH 6.5]). The filters were UV cross-linked by using

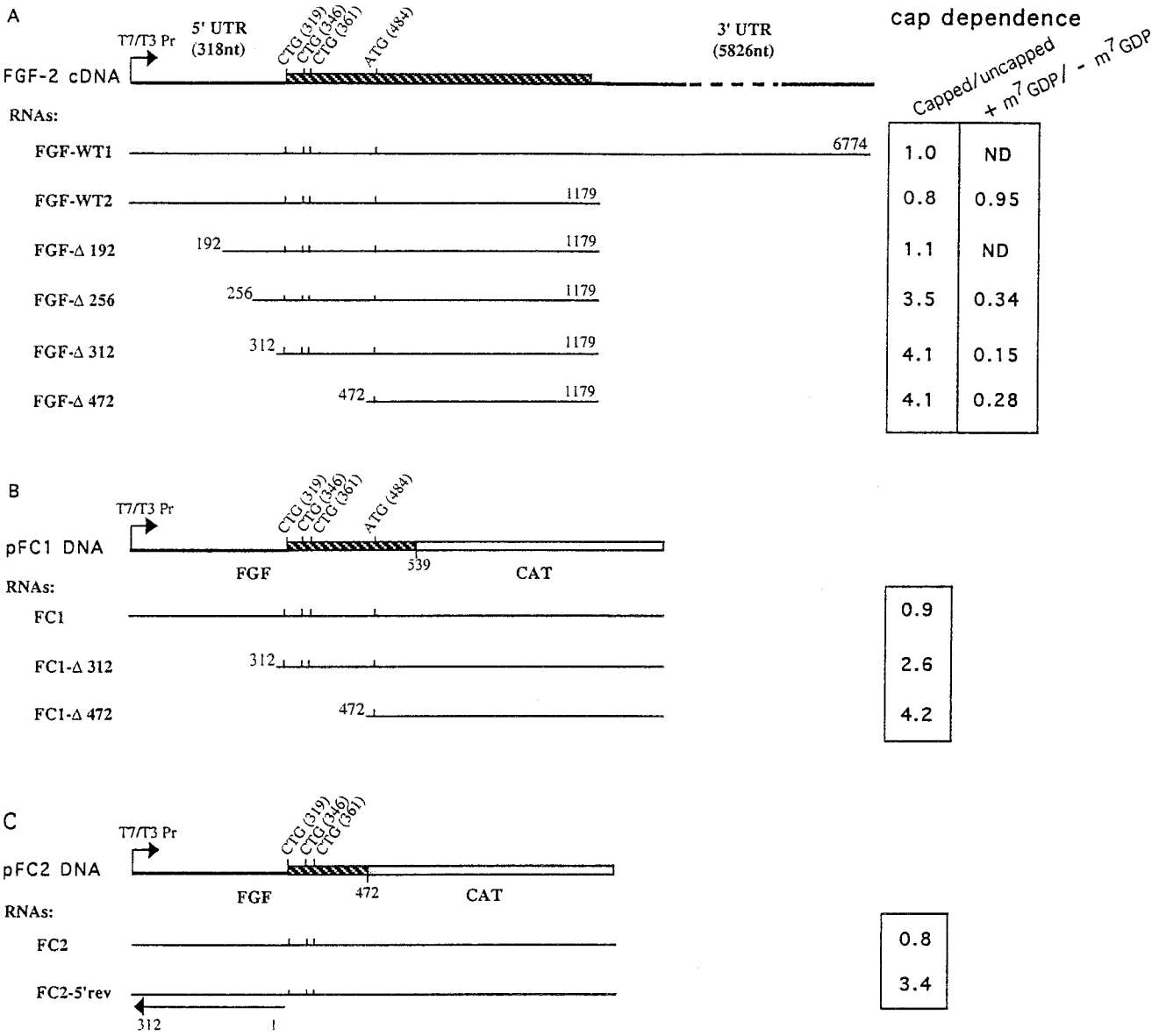

FIG. 1. (A) Schematic representation of the 6,774-nt-long FGF-2 cDNA (plasmid pSCT-FGF) and of full-length and deleted RNAs used for translation experiments. Full-length RNAs WT1 and WT2, corresponding to normal mRNA species, have 5,823- and 228-nt-long 3′ UTRs, respectively. 5′-deleted RNAs have the shorter 3′ UTR. Plasmid construction has been previously described (41). (B) Schematic representation of the chimeric construct FGF-CAT1 (plasmid pFC1) and of full-length and deleted RNAs used for translation experiments. Nucleotides 1 to 539 of FGF-2 cDNA were fused to the CAT coding sequence, retaining the four FGF-2 start codons. (C) Schematic representation of the chimeric construct FGF-CAT2 (plasmid pFC2) and of full-length and deleted RNAs used for translation experiments. Nucleotides 1 to 472 were fused to CAT, retaining the CTG codons but removing the ATG codon. Plasmid pFC2-5′rev resulted from inversion of sequence from nt 1 to 312 containing the 5′ UTR. Plasmid construction is described in Materials and Methods. On the right are summarized the results presented in Fig. 2 to 4. The effect of cap on global translation of each FGF or FGF-CAT mRNA is indicated. Capped/uncapped is the ratio of the translation efficiency of capped RNA to that of uncapped RNA. $+m^7GDP/-m^7GDP$ is the ratio of the translation efficiency of capped RNA in the presence of m^7GDP to that in the absence of m^7GDP.

a UV Stratalinker apparatus (Stratagene) at (254 nm and 120,000 μJ). Prehybridization of the filters was carried out for 2 h at 42°C in 50% formamide–5× SSC (1× SSC is 0.15 M NaCl plus 0.015 M sodium citrate [pH 7]–2× Denhardt's solution–0.1% SDS–100 μg of sonicated denatured salmon sperm DNA (Boehringer) per ml. Hybridization was performed under the same conditions with 10^7 cpm of probe per ml for 15 h at 42°C. Filters were washed for 15 min in 1× SSC–0.1% SDS at 20°C and then for 15 min with 0.2× SSC–0.1% SDS.

RESULTS

***cis*-acting sequences involved in cap-independent translation of FGF-2 mRNA.** To test whether translation of the FGF-2 mRNA could be cap independent, capped and uncapped FGF-2 RNAs with either the complete 483-nt-long leader sequence or progressive deletions from the 5′ end (Fig. 1A) were synthesized in vitro and compared for translation efficiency in RRL (Fig. 2).

The results showed that capped and uncapped FGF-2 mRNAs were translated with the same efficiency when they had either the complete leader sequence or a deletion of the first 192 nt (Fig. 2, lanes 1 to 6). This result was obtained whether the mRNA had a long (lanes 1 and 2) or short (lanes 3 and 4) 3′ UTR, both corresponding to FGF-2 mRNA species existing in cells (5, 55). In contrast, after removal of the first

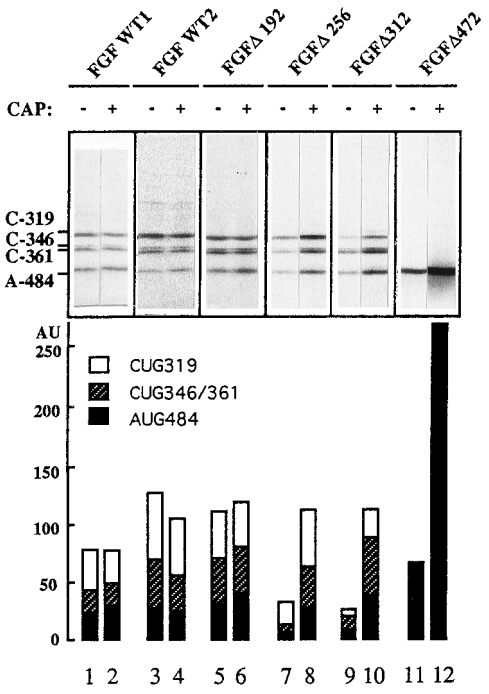

FIG. 2. Cap influence on FGF-2 mRNA translation in RRL. RNAs described in Fig. 1A were synthesized in vitro by using T7 RNA polymerase, with or without addition of m^7GpppG (0.5 mM) to the transcription reaction mixture, in order to obtain capped or uncapped RNA, respectively. Capped (+) and uncapped (−) mRNAs were translated in RRL at a concentration of 10 μg/ml, in the presence of [^{35}S]methionine (see Materials and Methods). Translation products were analyzed by electrophoresis on a 12.5% polyacrylamide gel and autoradiography of the gel. Start codons and sizes are indicated. The bands were quantitated by scanning autoradiograms with a BIOCOM apparatus. The relative values (in arbitrary units [AU]) are represented by histograms under the corresponding lanes. The results shown correspond to representative experiments that were repeated 5 to 10 times.

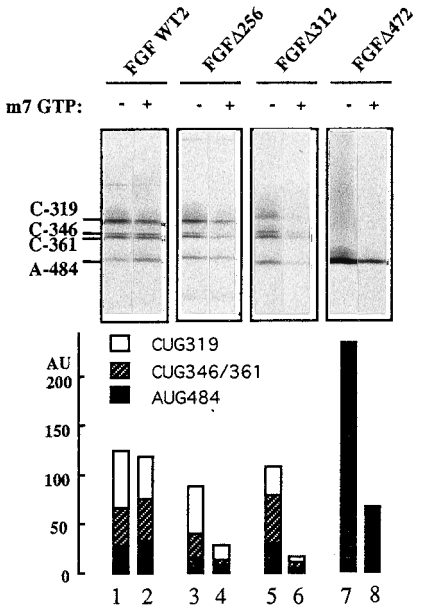

FIG. 3. Translation in RRL of the capped mRNAs used in Fig. 2 in the presence (+) or absence (−) of the cap analog m^7GDP (0.8 mM). Translation products were analyzed by polyacrylamide gel electrophoresis followed by autoradiography and quantitation of the bands as for Fig. 2. The results shown correspond to representative experiments that were repeated three to five times.

256 nt or more, capped RNAs were translated three to five times more efficiently than uncapped RNAs (lanes 7 to 12).

These results were confirmed by the use of a cap analog, 7-methyl GDP (m^7GDP), competing for the cap-binding factors (Fig. 3): addition of m^7GDP inhibited translation of RNAs with a deletion of 256 nt or more (lanes 3 to 8) but did not inhibit translation of the FGF-2 mRNA with a complete leader (lanes 1 and 2). These experiments indicate that translation initiation of FGF-2 mRNA is cap independent and that this process requires at least one element of the 5′ UTR, located between nt 192 and 256.

To further characterize the *cis*-acting sequences involved in cap-independent translation, different parts of the 5′ end of FGF-2 mRNA were fused with the CAT coding sequence. In pFC1 (Fig. 1B), the first 539 nt of FGF-2 mRNA were fused to CAT. Cell-free translation of FC1 RNA produced four chimeric proteins as expected following initiation at each start codon. The fusion pFC2 (Fig. 1C) was constructed by using nt 1 to 472 of FGF-2 mRNA, with the three CUG codons but without the AUG codon. Cell-free translation of FC2 RNA gave the expected chimeric proteins initiated at the CUG codons. Capped and uncapped FC1 and FC2 RNAs were translated with similar efficiencies, indicating that translation was cap independent for both RNAs (Fig. 4, lanes 1, 2, 7, and 8). As was observed with FGF-2 mRNA (Fig. 2), translation of the FGF-CAT chimeric RNAs became cap dependent after removal of nt 1 to 312 or 1 to 472 (Fig. 4, lanes 3 to 6). Furthermore, inversion of the 5′ 312 nt also rendered translation cap dependent (Fig. 4, lanes 9 and 10). According to the results presented in Fig. 2 to 4, the process of cap-independent translation did not involve RNA sequences located upstream of nt 192 or downstream of nt 472. This finding suggests that sequences located between nt 192 and 472 of the FGF-2 mRNA leader are sufficient, whereas sequences between nt 192 and 256 are necessary, to promote cap-independent initiation of translation.

Internal entry of ribosomes in the FGF-2 mRNA. Bicistronic vectors were used to determine any possible internal binding of ribosomes in FGF-2 mRNA (22, 38). In this system, two open reading frames (ORFs) are carried by the same mRNA, and in eukaryotic cells the second one cannot be translated unless there is internal ribosome entry between the first and second ORFs. We constructed a bicistronic vector with the CAT coding sequence as the first ORF and FGF-2 coding sequence preceded by the mRNA 5′ UTR as the second ORF (Fig. 5A, pBI-FGF). A stable hairpin was also introduced at the RNA 5′ end (pHP-FGF), which would be expected to down regulate ORF1 but not ORF2 if there was internal ribosome binding (32). COS-7 cells were transfected by the mono- and bicistronic vectors described in Fig. 5A. RNase mapping experiments allowed us to detect similar levels of RNA expression with all vectors (Fig. 5B, lanes 3 to 5), indicating that the 5′ hairpin did not affect RNA stability.

Translation of the monocistronic and bicistronic mRNAs was analyzed by Western immunoblotting with anti-CAT and anti-FGF-2 antibodies. Expression of CAT (ORF1) from the bicistronic mRNAs was three times less efficient in the presence of the 5′ hairpin (Fig. 6, lanes 2 and 3). In contrast, the four forms of FGF-2 (ORF2) were expressed with the same efficiency by the bicistronic mRNAs, whether they contained the hairpin or not. This efficiency, evaluated at 25% of that of the control monocistronic mRNA (Fig. 6, lanes 5 to 11), is discussed below. In conclusion, addition of a 5′ hairpin to the

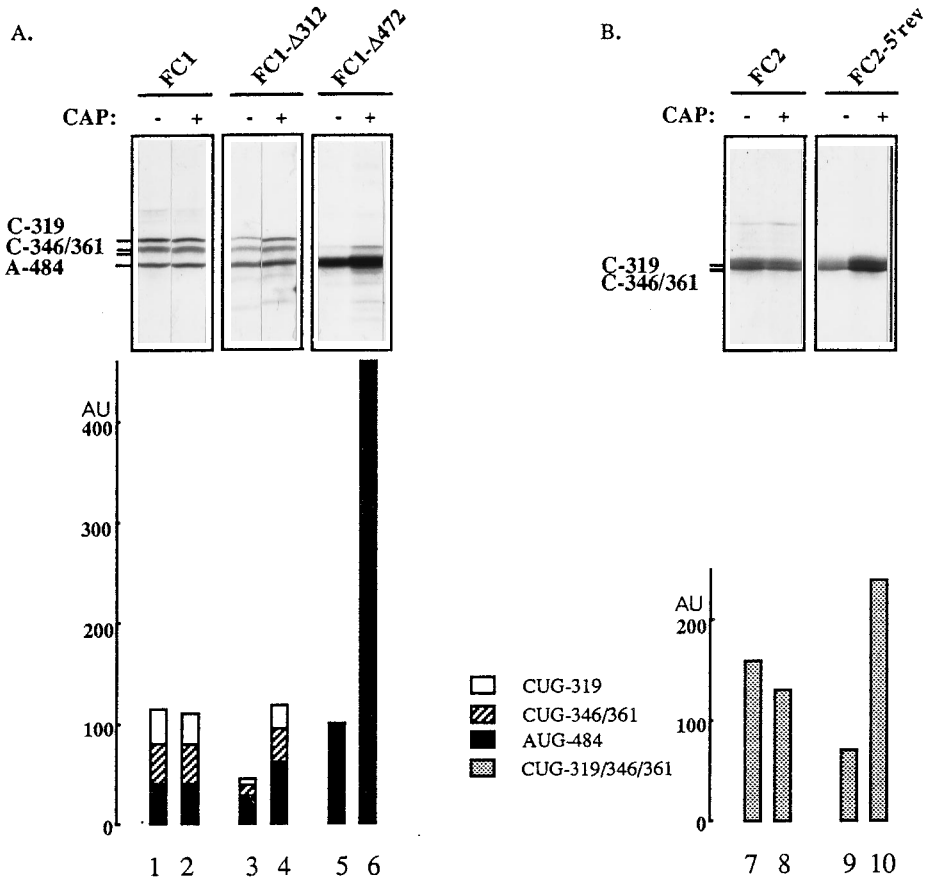

FIG. 4. Cap influence on translation of chimeric FGF-CAT mRNAs expressed from plasmids of the pFC1 and pFC2 series. RNAs described in Fig. 1B were synthesized as for Fig. 2. Capped (+) and uncapped (−) mRNAs were translated in RRL at a concentration of 10 μg/ml, in the presence of [^{35}S]methionine (see Materials and Methods). Translation products were analyzed by electrophoresis on a 12.5% polyacrylamide gel followed by autoradiography of the gel and quantitation of the bands as for Fig. 2. Start codons and sizes are indicated. The results shown correspond to representative experiments that were repeated three to five times. The additional band visible in lane 6 probably results from artifactual initiation at an in-frame ACG present in the polylinker.

bicistronic mRNA was able to affect expression of the first ORF (CAT) but did not affect expression of the second ORF (FGF-2). These results, which indicate that the FGF-2 mRNA can be translated in a cap-independent manner in vivo, strongly suggest the existence of an IRES in this mRNA.

Identification of an IRES between nt 154 and 319 of the FGF-2 mRNA 5′ UTR. The presence of an IRES in FGF-2 mRNA was further investigated by constructing different bicistronic vectors with the FGF-CAT fusions depicted in Fig. 1B as ORF2 (Fig. 7A). The originality of this strategy was that it allowed the detection of ORF1 and ORF2 products with a anti-CAT antibody on the same Western immunoblot, providing a direct comparison of the expression of both cistrons.

COS-7 cells were transfected by the bicistronic vectors (pBI and pHP series) containing FC1 and FC2 fusions as in Fig. 6. The integrity of the bicistronic FC1 RNA was verified by Northern blotting (Fig. 7B), allowing us to rule out the possibility of a cleavage or use of a cryptic promoter located between the two cistrons. Expression of the bicistronic RNAs FC1 and FC2 was analyzed by Western immunoblotting with the anti-CAT antibody.

In agreement with the data in Fig. 6, ORF2 was expressed in both fusions, with or without the 5′ hairpin (Fig. 7C, lanes 2, 3, 8, and 9). In contrast, ORF2 expression was not observed when the 5′ UTR was deleted (lanes 4 and 5) or inverted (lanes 6, 7, 10, and 11), as indicated by the absence of the FGF-CAT fusion proteins. These data, which fit perfectly with the cap dependence study presented in Fig. 4, confirmed the presence of an IRES in FGF-2 mRNA. Furthermore, they allowed us to localize this IRES in the 5′ UTR of the messenger.

An alternative strategy to localize the IRES was to introduce in-frame additional AUG codons into the 5′ UTR of FGF-2 mRNA (Fig. 8A). According to the ribosome scanning model, insertion of an efficient AUG codon is expected to extinguish downstream initiation codons. In contrast, if there is an IRES between the inserted AUG and the downstream initiation codons, we can expect that translation initiation at the downstream codons will not be abolished.

Constructs with an additional AUG either at position 319 or at position 154 were tested both by transfection of COS-7 cells (Fig. 8B) and by in vitro translation in RRL (Fig. 8C). As shown in Fig. 8B (lanes 4 and 5), insertion of an AUG at position 319 (replacing CUG1) completely abolished translation initiation at CUG2, CUG3, and AUG codons (positions 346, 361, and 184, respectively) in COS cells, as would be expected in the case of a ribosome scanning from position 319 to the downstream codons. In contrast, insertion of an AUG at position 154 did not extinguish translation initiation at the downstream codons (Fig. 8B, lanes 6 and 7).

Similar results were obtained in the RRL (Fig. 8C, lanes 3, 4, 5, and 6). However, in that translation system, initiation at the natural AUG (position 484) was not completely abolished

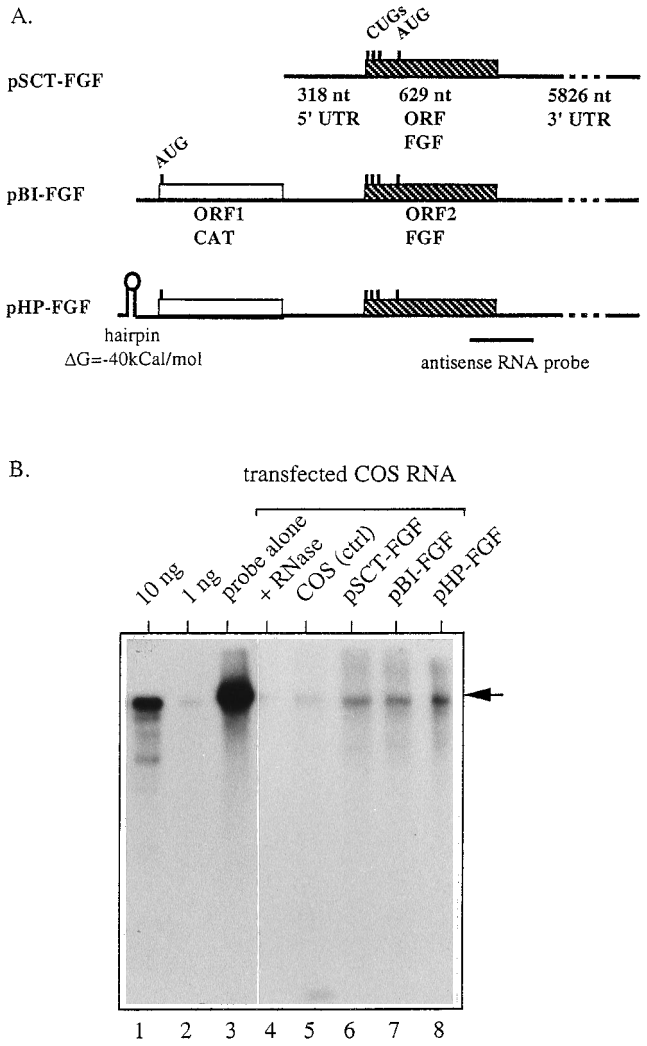

FIG. 5. (A) Schematic representation of the mono- and bicistronic vectors used for COS cell transfection for Fig. 5B and 6. Monocistronic plasmid pSCT-FGF contained the complete FGF-2 cDNA. Bicistronic plasmid pBI-FGF resulted from introduction into vector pSCT-CAT of FGF-2 cDNA downstream of the CAT ORF. Bicistronic plasmid pHP-FGF resulted from introduction of a stable hairpin (18 bp) into plasmid pBI-FGF 5′ of the CAT ORF. (B) Quantitation by RNase mapping of mono- and bicistronic FGF-2 RNAs obtained after COS cell transfection. COS-7 monkey cells were transiently transfected with the vectors described in Fig. 5A. At 48 h after transfection, total cellular RNAs were purified and analyzed by RNase protection (lanes 3 to 5). RNase A and T_1 protection was performed as described in Materials and Methods with a T7 RNA probe complementary to the FGF-2 coding sequence (nt 889 to 1179), which is depicted in Fig. 5A. Nontransfected COS cells were used as a negative control (ctrl). We checked that the reaction was quantitative by using two concentrations (10 and 1 ng) of RNA synthesized in vitro (lanes 6 and 7). Lanes 1 to 5 correspond to a 24-h exposure, whereas lanes 6 to 8 correspond to a 4-h exposure of the same gel.

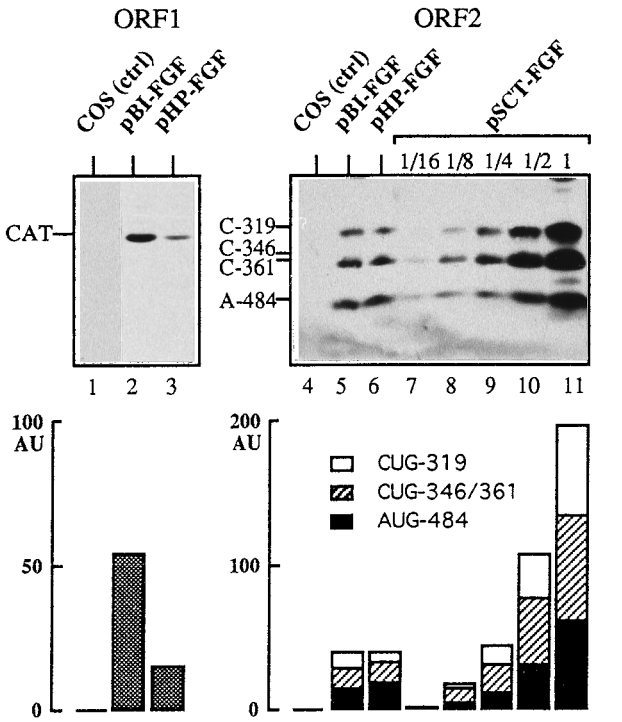

FIG. 6. Expression of monocistronic and bicistronic FGF-2 mRNAs in transfected COS-7 monkey cells. COS-7 monkey cells were transiently transfected with plasmids pSCT-FGF, pBI-FGF, and pHP-FGF. Cell extracts were analyzed by Western immunoblotting (3 μg of total protein per lane), using an anti-CAT (lanes 1 to 3) or anti-FGF-2 (lanes 4 to 11) antibody as described in Materials and Methods. To compare initiation levels at the FGF-2 codons obtained with mono- and bicistronic constructs, the cell extract obtained from transfection with the monocistronic plasmid pSCT-FGF was diluted 2-, 4-, 8-, or 16-fold (as indicated for lanes 7 to 11). The results shown correspond to representative experiments that were repeated at least five times. The control (ctrl) lanes correspond to mock-transfected COS cells (lanes 1 and 4). The lanes corresponding to pBI-FGF and pHP-FGF are indicated. Positions of migration of CAT (ORF1) and of the different isoforms of FGF-2 (ORF2) are indicated. Bands were scanned with a BIOCOM apparatus, and their relative intensities (in arbitrary units [AU]) are represented by histograms under the corresponding lanes.

by the presence of an additional AUG at position 319 (lanes 3 and 4).

These observations, in correlation with the cap dependence experiments (Fig. 2), suggested a localization of the IRES between nt 154 and 319 of FGF-2 mRNA.

DISCUSSION

The results reported here, together with those of previous studies (41), strongly suggest that FGF-2 synthesis is regulated at the translational level. Recently, we have demonstrated the existence of *cis*-regulatory elements in the mRNA leader (41). Here we provide evidence that FGF-2 is synthesized through a mechanism of internal initiation of translation. The 5′ UTR sequence required for cap-independent translation corresponds to an element previously described for its ability to inhibit translation in wheat germ extract but not in RRL and COS cells (41). This finding suggests that *trans*-acting factors, lacking in wheat germ, may control internal ribosome entry in mammalian systems. Furthermore, synthesis of AUG-initiated FGF-2, the overexpression of which can induce cell transformation (11), seems to be regulated by a double-locking mechanism: (i) internal ribosome entry depending on a 5′ UTR element and (ii) strong inhibition by a *cis* element identified in the alternatively translated region, upstream of the AUG codon (41).

One criticism with respect to our results is the possibility that we are examining some form of reinitiation occurring at ORF2 after translation of ORF1. In that case, the 5′rev construct might disrupt this hypothetical reinitiation by introducing out-of-frame AUGs between ORF1 and ORF2. However, we can rule out that possibility, as the 5′rev construct introduces only one AUG in a bad context whereas it removes two out-of-frame AUGs that are present at positions 108 and 117 from the

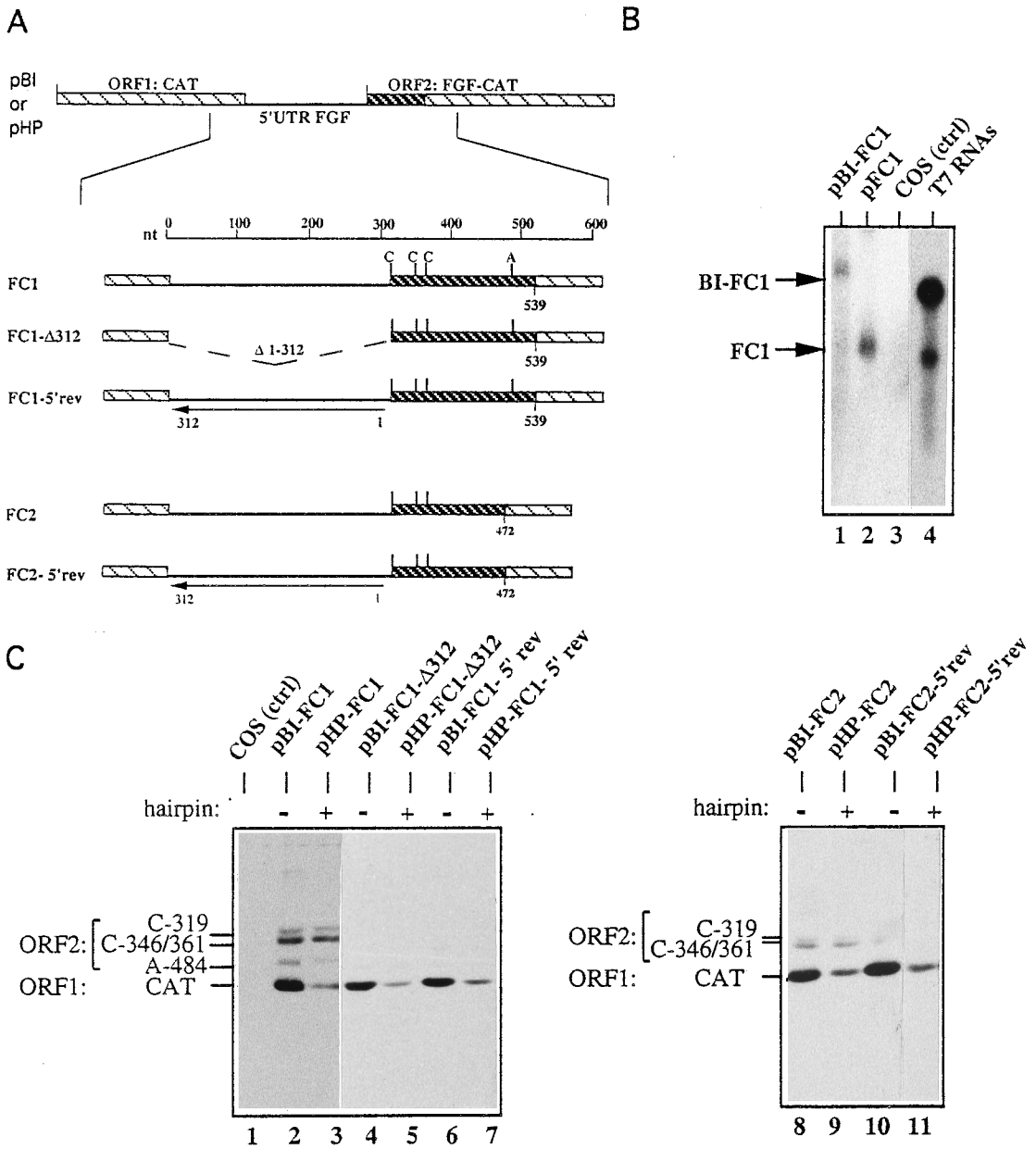

FIG. 7. Expression of bicistronic FGF-CAT chimeric mRNAs in COS-7 cells. (A) Schematic representation of the chimeric constructs. Fusions FGF-CAT1 and FGF-CAT2 (described in Fig. 2), having a complete, deleted, or inverted 5′ UTR (FC, FC-Δ312, or FC-5′rev, respectively), were used to construct bicistronic vectors with or without a stable hairpin 5′ of ORF1. (B) Northern blotting of monocistronic and bicistronic RNAs. COS-7 cells were transfected with mono- and bicistronic vectors pFC1 and pBI-FC1 encoding the FGF-CAT1 fusion. Total RNAs were purified as for Fig. 5B and assayed by Northern blotting as described in Materials and Methods, using a ^{32}P-labelled DNA probe corresponding to the CAT coding sequence (lanes 1 and 2). Lane 3 corresponds to mock-transfected (control [ctrl]) COS cells. In vitro-synthesized FC1 and BI-FC1 RNAs were used as a size control (lane 4). The difference in migration of T7 and COS RNAs is due to the absence of polyadenylation of T7 RNAs. Lanes 1 to 3 correspond to a 16-h exposure, whereas lane 4 corresponds to a 2-h exposure of the same filter. (C) Transfection of COS-7 cells by the different bicistronic constructs depicted in Fig. 7A. Cell extracts were analyzed as for Fig. 6 by Western immunoblotting using an anti-CAT antibody, allowing the simultaneous detection of both products from ORF1 and from ORF2. Lane 1 corresponds to mock-transfected (control [ctrl]) COS cells. Transfections with bicistronic vectors pBI and pHP, without or with the 5′ hairpin (indicated by − or +), are as indicated above the lanes. The bands corresponding to CAT (ORF1) and FGF-CAT (ORF2), as well as the different initiation codons, are indicated. These experiments were repeated 5 to 10 times. The left and right panels correspond to transfection with plasmids of the pFC1 and pFC2 series, respectively.

FGF-2 mRNA 5′ end. Furthermore, the absence of ORF2 expression with the deletion of nt 1 to 312 cannot be explained by disruption of reinitiation by bringing the two ORFs close together, since the intercistronic distance in this construct is still 110 nt.

We also wish to discuss the question of RNA cleavage between the two ORFs that would lead to a population of RNAs with a 5′ end upstream of the second ORF. It is clear in Fig. 7B that such a population of RNAs is not present at a detectable level. Furthermore, the literature provides us with several arguments to answer this question (3): (i) RNA capping occurs by condensation of pG from GTP on either the diphosphate or triphosphate 5′ end, whereas a cleaved RNA would have a monophosphate or a hydroxyl 5′ end, (ii) the posttranscrip-

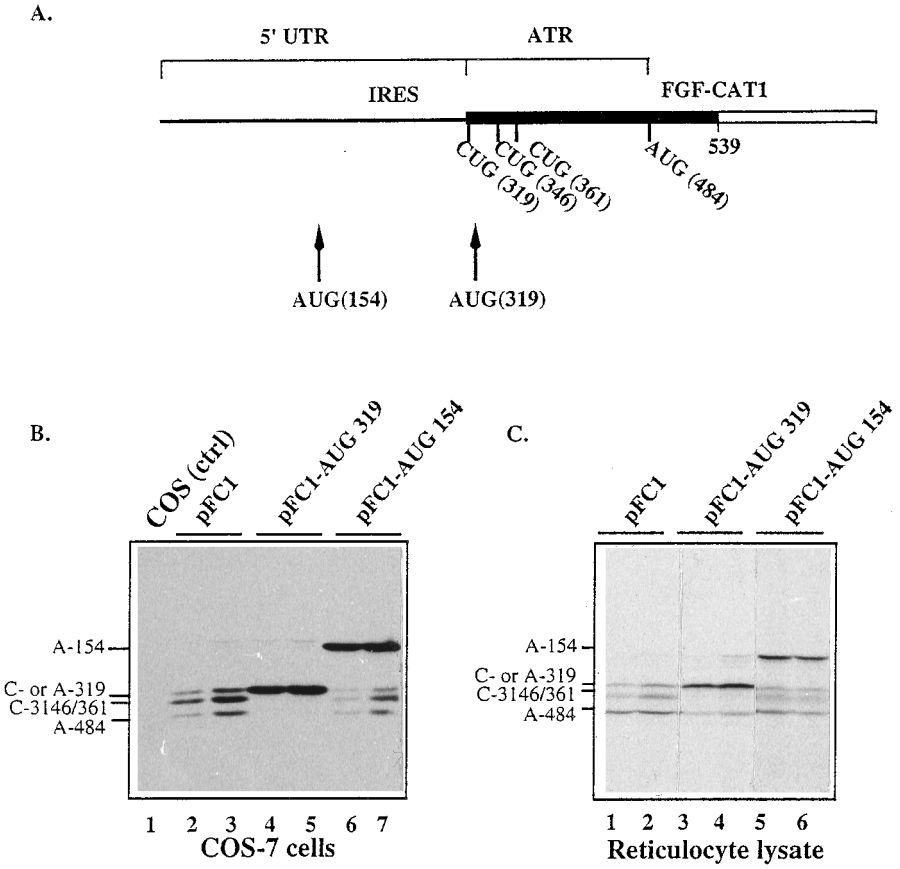

FIG. 8. Expression of monocistronic FGF-CAT mRNAs with AUG insertions upstream or downstream of the IRES. (A) Schematic representation of the leader sequence of FGF-2 mRNA, showing the 5′ UTR and the alternatively translated region (ATR). AUG codons (arrows) were introduced by site-directed mutagenesis at position 154 or 319 (see Materials and Methods). (B) COS-7 cells were transfected by plasmid pFC1 as well as by plasmids with ATG insertions (pFC1-ATG319 and pFC1-ATG154). Transfections were performed with 0.5 (lanes 2, 4, and 6) and 1 (lanes 3, 5, and 7) μg of each plasmid per ml. Western immunoblotting was carried out as for Fig. 7. (C) In vitro transcriptions were performed with the three plasmids used for panel B. Translation of RNAs in the RRL was carried out as for Fig. 2, using 5 (lanes 1, 3, and 5) and 15 (lanes 2, 4, and 6) μg of each RNA species per ml. We always observed a saturation of the translation system with 5 to 10 μg of RNA per ml, whereas it was expected not to saturate up to about 30 μg of RNA per ml. This feature, characteristic of RNAs with the FGF-2 5′ UTR, remains unexplained.

tional capping does not occur at detectable levels, and (iii) capping and transcription initiation are tightly linked processes. Knowing that the cap is important not only for translation initiation but also for RNA stability and export from the nucleus, a hypothetical undetectable population of uncapped cleaved RNAs with ORF2 cannot be responsible for the ORF2 expression observed with the bicistronic vectors, which is 25% of that of the corresponding monocistronic vectors (Fig. 6). A similar reasoning allows us to rule out the possibility of a cleavage between the two cistrons that would lead to expression of ORF1 alone in our constructs with a deleted or inverted 5′ UTR (Δ312 or 5′rev). Such a cleaved nonpolyadenylated RNA, improbable since it is not detected with the pBI-FC1 construct (Fig. 7B), would be unstable and unefficiently translated; thus, it cannot account for the ORF1 expression observed in Fig. 7C.

Why are the FGF-2 initiation codons in the bicistronic mRNA used at only 25% of their efficiency in the monocistronic mRNA? Several explanations can be given for such a difference. First, the IRES element may be affected by long-range tertiary interactions and consequently function differently depending on its location in the RNA. Moreover, ongoing translation of the first cistron may alter the structure of the IRES and affect the translational efficiency of the second cistron (35). Another possibility is that competition between the two cistrons for initiation factors is responsible for the different efficiencies of the mono- and bicistronic RNAs. Alternatively, the low efficiency of the bicistronic RNA may also indicate that both mechanisms of ribosome scanning from the 5′ end and internal binding are involved in translation of the FGF-2 mRNA. Thus, the balance between these two processes may be an ingenious mechanism able to control the alternative initiation of translation, which could extend to other mRNAs possessing alternative start codons.

A molecular mechanism for internal ribosome binding on picornavirus mRNA has emerged, resulting from the identification of a *cis* element, an oligopyrimidine tract, highly conserved among picornaviruses and necessary for internal initiation of translation (23, 33, 39). It has been proposed that this pyrimidine stretch, located upstream from an appropriately spaced AUG, could be analogous to the prokaryotic Shine-Dalgarno sequence. Indeed, it shows sequences complementary to purine stretches in mammalian 18S rRNA. Furthermore, the requirement of larger sequences in the picornavirus 5′ UTR for internal initiation of translation suggests that the interaction of 40S ribosomes with this region, via 18S rRNA or *trans*-acting factors, also involves a global superstructure (33). However, in the case of FGF-2 mRNA, there is no pyrimidine stretch in the 5′ UTR, indicating that the *cis* elements allowing internal ribosome binding on FGF-2 mRNA are probably dif-

ferent from that identified for picornavirus. Moreover, there is no homology between any portion of the G+C-rich 5′ UTR of FGF-2 mRNA and the 55-nt-long Antennapedia IRES (36), which is A rich. In contrast, sequence similarity could be found between the 5′ UTRs of FGF-2 and immunoglobulin heavy-chain-binding protein mRNAs, which are both GC rich (42, 53). Thus, the process of internal ribosome entry of FGF-2 mRNA may depend on mammalian specific *trans*-acting factors.

The FGF-2 mRNA is translated by a process of alternative initiation, using three noncanonical CUG codons and one AUG codon. This feature differentiates it from the other known cellular messengers containing an IRES. Indeed, the alternative use of the different codons determines the localization and probably the target of FGF-2 in the cell (9, 11). Strikingly, the IRES identified in this report is located in the 5′ UTR, upstream of the four initiation codons, whereas it would have seemed logical to find an IRES in the alternatively translated region, between the CUG3 and AUG codons. Thus, in these conditions, the process of ribosome internal entry does not regulate the relative use of the four initiation codons. However, the existence of a second IRES in the alternatively translated region cannot be ruled out, as shown by the results obtained in RRL with AUG insertion (Fig. 8C, lanes 3 and 4). This second IRES, the use of which would depend on the translation system, has been already suggested in a report in which we have shown that mutation of the three CUG into nonstart codons does not result in enhancement of initiation at the AUG codon (41). The existence of cells producing mostly the AUG-initiated form of FGF-2 (39a) will be very useful for resolving this question.

The process of internal ribosome entry could allow FGF-2 mRNA translation when eIF-4E-dependent initiation is inhibited, as happens in mitosis or under stress conditions (6, 37). eIF-4E plays a central role in the control of cell growth and is activated by growth factors and mitogenic agents (15, 16). Thus, the process of internal translation initiation, independent of eIF-4E and probably controlled by specific *trans*-acting factors, would be able to induce an autoparacrine loop: under conditions of cell growth arrest or in response to stress, when there is very little active eIF-4E, FGF-2 could be specifically synthesized by the internal initiation pathway. Production of the growth factor would result in activation of eIF-4E (15, 16), derepression of translation, and stimulation of cell proliferation or differentiation (31). This could play a key role in wound healing or tumor neovascularization processes.

ACKNOWLEDGMENTS

We thank B. Bugler for helpful discussions, M. Allouche, C. Dickson, and J. C. Faye for reading the manuscript, and D. Warwick for English proofreading.

This work was supported by grants from the Institut National de la Santé et de la Recherche Médicale, Association Pour la Recherche Contre le Cancer, and Conseil Régional Midi-Pyrénées. S. Vagner has a fellowship from the Ministère de la Recherche et de l'Enseignement.

REFERENCES

1. **Acland, P., M. Dixon, G. Peters, and C. Dickson.** 1990. Subcellular fate of the *Int-2* oncoprotein is determined by choice of initiation codon. Nature (London) **343:**662–665.
2. **Bandyopadhyay, P. K., C. Wang, and H. L. Lipton.** 1992. Cap-independent translation by the 5′ untranslated region of Theiler's murine encephalomyelitis virus. J. Virol. **66:**6249–6256.
3. **Banerjee, A. K.** 1980. 5′-terminal cap structure in eukaryotic messenger ribonucleic acids. Microbiol. Rev. **44:**175–205.
4. **Belsham, G. J., and J. K. Brangwyn.** 1990. A region of the 5′ noncoding region of foot-and-mouth disease virus RNA directs efficient internal initiation of protein synthesis within cells; involvement with the role of the L protease in translational control. J. Virol. **64:**5389–5395.
5. **Bensaid, M., F. Malecaze, H. Prats, F. Bayard, and J. P. Tauber.** 1989. Autocrine regulation of bovine retinal capillary endothelial cells (BREC) proliferation by BREC derived fibroblast growth factor. Exp. Eye Res. **45:** 801–813.
6. **Bonneau, A., and N. Sonenberg.** 1987. Involvement of the 24-kDa cap-binding protein in regulation of protein synthesis in mitosis. J. Biol. Chem. **262:**11134–11139.
7. **Borman, A., and R. J. Jackson.** 1992. Initiation of translation of human rhinovirus RNA: mapping the internal ribosome entry site. Virology **188:** 685–696.
8. **Brigstock, D. R., J. Sasse, and M. Klagsbrun.** 1991. Subcellular distribution of basic fibroblast growth factor in human hepatoma cells. Growth Factors **4:**189–196.
9. **Bugler, B., F. Amalric, and H. Prats.** 1991. Alternative initiation of translation determines cytoplasmic or nuclear localization of basic fibroblast growth factor. Mol. Cell. Biol. **11:**573–577.
10. **Chomczynski, P., and N. Sacchi.** 1987. Single-step method of RNA isolation by acid guanidinium thiocyanate-phenol-chloroform extraction. Anal. Biochem. **162:**156–159.
11. **Couderc, B., H. Prats, F. Bayard, and F. Amalric.** 1991. Potential oncogenic effects of basic fibroblast growth factor requires cooperation between CUG and AUG-initiated forms. Cell Regul. **2:**709–718.
12. **de Benedetti, A., and R. E. Rhoads.** 1990. Overexpression of eukaryotic protein synthesis initiation factor 4E in HeLa cells results in aberrant growth and morphology. Proc. Natl. Acad. Sci. USA **87:**8212–8216.
13. **Duncan, R., S. C. Milburn, and J. W. B. Hershey.** 1987. Regulated phosphorylation and low abundance of HeLa cell initiation factor eIF-4E suggest a role in translational control. J. Biol. Chem. **262:**380–388.
14. **Florkiewicz, R. Z., and A. Sommer.** 1989. Human basic fibroblast growth factor gene encodes four polypeptides: three initiate translation from non-AUG codons. Proc. Natl. Acad. Sci. USA **86:**3978–3981.
15. **Frederickson, R. M., K. S. Montine, and N. Sonenberg.** 1991. Phosphorylation of eukaryotic initiation factor 4E is increased in *Src*-transformed cell lines. Mol. Cell. Biol. **11:**2896–2900.
16. **Frederickson, R. M., W. E. Mushynski, and N. Sonenberg.** 1992. Phosphorylation of translation initiation factor eIF-4E is induced in a *ras*-dependent manner during nerve growth factor-mediated PC12 cell differentiation. Mol. Cell. Biol. **12:**1239–1247.
17. **Glass, M. J., X. Y. Jia, and D. F. Summers.** 1993. Identification of the hepatitis-A virus internal ribosome entry site—invivo and invitro analysis of bicistronic RNAs containing the HAV 5′ noncoding region. Virology **193:** 842–852.
18. **Gospodarowicz, D., G. Neufeld, and L. Schweigerer.** 1986. Fibroblast growth factor. Mol. Cell. Endocrinol. **46:**187–204.
19. **Hiremath, L. S., N. R. Webb, and R. E. Rhoads.** 1985. Immunological detection of the messenger RNA cap-binding protein. J. Biol. Chem. **260:** 7843–7849.
20. **Jackson, R. J.** 1988. Picornavirus break the rules. Nature (London) **334:**292–293.
21. **Jang, S. K., M. V. Davies, R. J. Kaufman, and E. Wimmer.** 1989. Initiation of protein synthesis by internal entry of ribosomes into the 5′ nontranslated region of encephalomyocarditis virus RNA in vivo. J. Virol. **63:**1651–1660.
22. **Jang, S. K., H. Krausslich, M. J. H. Nicklin, G. M. Duke, A. C. Palmenberg, and E. Wimmer.** 1988. A segment of the 5′ nontranslated region of encephalomyocarditis virus RNA directs internal entry of ribosomes during in vitro translation. J. Virol. **62:**2636–2643.
23. **Jang, S. K., and E. Wimmer.** 1990. Cap-independent translation of encephalomyocarditis virus RNA: structural elements of the internal ribosomal entry site and involvement of a cellular 57-kD RNA-binding protein. Genes Dev. **4:**1560–1572.
24. **Kaminski, A., M. T. Howell, and R. J. Jackson.** 1990. Initiation of encephalomyocarditis virus RNA translation: the authentic initiation site is not selected by a scanning mechanism. EMBO J. **9:**3753–3759.
25. **Kandel, J., E. Bossy-Wetzel, F. Radvanyi, M. Klagsbrun, J. Folkman, and D. Hanahan.** 1991. Neovascularisation is associated with a switch to the export of bFGF in the multistep development of fibrosarcoma. Cell **66:**1095–1104.
26. **Koromilas, A. E., A. Lazaris-Karatzas, and N. Sonenberg.** 1992. Messenger RNAs containing extensive secondary structure in their 5′ non-coding region translate efficiently in cells overexpressing initiation factor-eIF-4E. EMBO J. **11:**4153–4158.
27. **Kozak, M.** 1978. How do eucaryotic ribosomes select initiation regions in messenger RNA? Cell **15:**1109–1123.
28. **Kozak, M.** 1991. An analysis of vertebrate mRNA sequences: intimations of translation control. J. Cell Biol. **115:**887–903.
29. **Kühn, R., N. Luz, and E. Beck.** 1990. Functional analysis of the internal translation initiation site of foot-and-mouth disease virus. J. Virol. **64:**4625–4631.
30. **Lazaris-Karatzas, A., K. S. Montine, and N. Sonenberg.** 1990. Malignant transformation by a eukaryotic initiation factor subunit that binds to mRNA 5′ cap. Nature (London) **345:**544–547.
31. **Lazaris-Karatzas, A., M. R. Smith, R. M. Frederickson, M. L. Jaramillo, Y.**

Liu, H. Kung, and N. Sonenberg. 1992. Ras mediates translation initiation factor 4E-induced malignant transformation. Genes Dev. **6:**1631–1642.
32. **Macejak, D. J., and P. Sarnow.** 1991. Internal initiation of translation mediated by the 5′ leader of a cellular mRNA. Nature (London) **353:**90–94.
33. **Meerovitch, K., R. Nicholson, and N. Sonenberg.** 1991. In vitro mutational analysis of *cis*-acting RNA translational elements within the poliovirus type 2 5′ untranslated region. J. Virol. **65:**5895–5901.
34. **Meerovitch, K., J. Pelletier, and N. Sonenberg.** 1989. A cellular protein that binds to the 5′-noncoding region of poliovirus RNA: implications for internal translation initiation. Genes Dev. **3:**1026–1034.
35. **Oh, S.-K., and P. Sarnow.** 1993. Gene regulation: translational initiation by internal ribosome binding. Curr. Opin. Gen. Dev. **3:**295–300.
36. **Oh, S.-K., M. P. Scott, and P. Sarnow.** 1992. Homeotic gene Antennapedia mRNA contains 5′-noncoding sequences that confer translational initiation by internal ribosome binding. Genes Dev. **6:**1643–1653.
37. **Panniers, R., E. B. Steward, W. C. Merrick, and E. C. Henshaw.** 1985. Mechanism of inhibition of polypeptide chain initiation in heat-shocked Ehrlich cells involves reduction of eukaryotic initiation factor 4F activity. J. Biol. Chem. **260:**9648–9653.
38. **Pelletier, J., and N. Sonenberg.** 1988. Internal initiation of translation of eukaryotic mRNA directed by a sequence derived from poliovirus RNA. Nature (London) **334:**320–325.
39. **Pilipenko, E. V., A. P. Gmyl, S. V. Maslova, Y. V. Svitkin, A. N. Sinyakov, and V. I. Agol.** 1992. Prokaryotic-like cis elements in the cap-independent internal initiation of translation on picornavirus RNA. Cell **68:**119–131.
39a. **Prats, A.-C.** Unpublished data.
40. **Prats, A. C., G. De Billy, P. Wang, and J. L. Darlix.** 1989. CUG initiation codon used for the synthesis of a cell surface antigen coded by the murine leukemia virus. J. Mol. Biol. **205:**363–372.
41. **Prats, A. C., S. Vagner, H. Prats, and F. Amalric.** 1992. *cis*-acting elements involved in the alternative translation initiation process of human basic fibroblast growth factor. Mol. Cell. Biol. **12:**4796–4805.
42. **Prats, H., M. Kaghad, A. C. Prats, M. Klagsbrun, J. M. Lélias, P. Liauzun, P. Chalon, J. P. Tauber, F. Amalric, J. A. Smith, and D. Caput.** 1989. High molecular mass forms of basic fibroblast growth factor are initiated by alternative CUG codons. Proc. Natl. Acad. Sci. USA **86:**1836–1840.
43. **Quarto, N., D. Talarico, R. Florkiewicz, and D. B. Rifkin.** 1991. Selective expression of high molecular weight basic fibroblast growth factor confers a unique phenotype to NIH 3T3 cells. Cell Regul. **2:**699–708.
44. **Renko, M., N. Quarto, T. Morimoto, and D. B. Rifkin.** 1990. Nuclear and cytoplasmic localization of different basic fibroblast growth factor species. J. Cell. Physiol. **144:**108–114.
45. **Rifkin, D. B., and D. Moscatelli.** 1989. Recent developments in the cell biology of fibroblast growth factor. J. Cell Biol. **109:**1–6.
46. **Rusconi, S., Y. Severne, O. Georgiev, I. Galli, and S. Wieland.** 1990. A novel expression assay to study transcriptional activators. Gene **89:**211–221.
47. **Sambrook, J., E. F. Fritsch, and T. Maniatis.** 1989. Molecular cloning: a laboratory manual, 2nd ed. Cold Spring Harbor Laboratory, Cold Spring Harbor, N.Y.
48. **Schweigerer, L., G. Neufeld, J. Friedman, J. A. Abraham, J. C. Fiddes, and D. Gospodarowicz.** 1987. Capillary endothelial cells express basic fibroblast growth factor, a mitogen that promotes their own growth. Nature (London) **325:**257–259.
49. **Slusher, L. B., E. C. Gillman, N. C. Martin, and A. K. Hopper.** 1991. mRNA leader length and initiation codon context determine alternative AUG selection for the yeast gene MOD5. Proc. Natl. Acad. Sci. USA **88:**9789–9793.
50. **Sonenberg, N.** 1988. Cap-binding proteins of eukaryotic messenger RNA: functions in initiation and control of translation. Prog. Nucleic Acid Res. Mol. Biol. **35:**173–297.
51. **Thach, R. E.** 1992. Cap recap: the involvement of eIF-4F in regulating gene expression. Cell **68:**177–180.
52. **Thomas, A. M., E. ter Haar, J. Wellink, and H. O. Voorma.** 1991. Cowpea mosaic virus middle component RNA contains a sequence that allows internal binding of ribosomes and that requires eukaryotic initiation factor 4F for optimal translation. J. Virol. **65:**2953–2959.
53. **Ting, J., and A. S. Lee.** 1988. Human gene encoding the 78000-dalton glucose-regulated protein and its pseudogene: structure, conservation, and regulation. DNA **7:**275–286.
54. **Tsukiyama-Kohara, K., N. Lizuka, M. Kohara, and A. Nomoto.** 1992. Internal ribosome entry site within hepatitis C virus RNA. J. Virol. **66:**1476–1483.
55. **Weich, H. A., N. Iberg, M. Klagsbrun, and J. Folkman.** 1990. Expression of acidic and basic fibroblast growth factors in human and bovine vascular smooth muscle cells. Growth Factors **2:**313–320.
56. **Yanagisawa-Miwa, A., Y. Uchida, F. Nakamura, T. Tomaru, H. Kido, T. Kamijo, T. Sugimoto, K. Kaji, M. Utsuyama, C. Kurashima, and H. Ito.** 1992. Salvage of infarcted myocardium by angiogenic action of basic fibroblast growth factor. Science **257:**1401–1403.